Ratio model serves suprathreshold color–luminance discrimination

Marcel J. Sankeralli and Kathy T. Mullen

McGill Vision Research, Department of Ophthalmology, McGill University, Montreal H3A 1A1, Canada

Trevor J. Hine

School of Applied Psychology, Faculty of Health Science, Griffith University, Brisbane, Queensland 4111, Australia, and McGill Vision Research, Department of Ophthalmology, McGill University, Montreal H3A 1A1, Canada

Received February 6, 2001; revised manuscript received July 6, 2001; accepted August 2, 2001

We extended earlier results [J. Opt. Soc. Am. A **16**, 2625 (1999)] to examine how the responses of the three postreceptoral mechanisms are combined to subserve discrimination of suprathreshold stimuli. Test thresholds were obtained in the presence of suprathreshold pedestals selected in different quadrants of the red–green/luminance and blue–yellow/luminance planes of cardinal color space. We showed that (1) test threshold was directly proportional to pedestal contrast for pedestal contrasts exceeding five times pedestal contrast threshold, and (2) there were exceptions to this proportionality, notably when the test and pedestal directions were fixed in the cardinal directions. Results support a ratio model of suprathreshold color–luminance discrimination, in which discrimination depends on a ratio of outputs of the postreceptoral mechanisms. We also observed that when test threshold was measured as a function of test color-space direction, masking by the achromatic component of the pedestal was less than that by the chromatic component. In addition, masking by a dark (negative luminance component) pedestal was lower than masking by a light (positive luminance) pedestal of a similar contrast. Our results demonstrated that (1) there is no fundamental difference between discrimination in the isoluminant and in the two chromoluminant cardinal planes, (2) there exists the possibility that discrimination in cardinal directions differs from that in noncardinal (intermediate) directions, and (3) suprathreshold discrimination of luminance differences may be more sensitive than that of chromatic differences for a given suprathreshold pedestal.

OCIS codes: 330.0330, 330.1720, 330.1800.

1. INTRODUCTION

The study of chromatic and luminance mechanism interactions has focused on the manner in which these mechanisms contribute jointly to contrast detection[1,2] or to masking.[3,4] The consensus from these studies is that the detection of jointly chromatic (isoluminant) and achromatic (luminance) stimuli (termed chromoluminant[5,6]) is achieved by distinct luminance and chromatic (red–green and blue–yellow) mechanisms, and that overall stimulus detectability is determined by a nonlinear summation of the responses of these respective detection mechanisms. It remains an open question how the responses of the detection mechanisms contribute to discrimination between chromoluminant stimuli at suprathreshold levels. One description of such discrimination, based on line-element models, suggests that threshold detection of the net chromatic and luminance difference is constant and independent of the pedestals on which these stimuli are superimposed. Wandell,[7] for example, proposed that discrimination may follow a line-element model for isoluminant stimuli, whereas discrimination of chromoluminant stimuli is mediated by discrete categorization, in which discrimination occurs when the two stimuli are on either side of a predefined perceptual boundary. This particular model, therefore, postulated a fundamental difference between isoluminant and chromoluminant discrimination. As opposed to line-element models, a more recent description[5,6] proposes a multistage interaction including cross-mechanism divisive inhibition, which is applicable in both isoluminant and chromoluminant conditions (see Section 4).

In the present study, we examine a parsimonious model consistent with the latter multistage description. This model asserts that discrimination thresholds at high pedestal contrasts are determined by the ratio of the outputs of the two postreceptoral mechanisms involved. We extend the results of our previous study[8] in which we investigated suprathreshold discrimination in the isoluminant plane. In that study, we measured the detection threshold of a hue increment, defined by a vector difference that lies orthogonal to a fixed pedestal direction in cardinal space. This was performed on the assumption that suprathreshold discrimination could be resolved into two separable components, perpendicular and parallel to the pedestal direction (reflecting hue and contrast changes, respectively). We observed that hue-increment thresholds obeyed a ratio model, stating that, for pedestal contrasts exceeding a certain value (~5 times pedestal detection threshold), the hue-increment threshold was directly proportional to the pedestal contrast. In the present study, we perform a similar measurement in the two other cardinal planes: the plane defined by the red–green and luminance axes and that defined by the blue–yellow and luminance axes. We observe a similar result

0740-3232/2002/030425-11$15.00

in these two planes, and conclude that discrimination of isoluminant differences and that of chromoluminant differences are governed by similar rules.

2. METHODS

A. Apparatus

Visual stimuli were presented on a Barco 7651 RGB monitor driven by a Cambridge Research Systems VSG2/1 video controller interfaced with a Gateway 2000 (Pentium) computer. Linearization of the outputs of the three phosphors was achieved by using a double calibration procedure: the first calibration taking account of the gamma-function voltage-luminance characteristic for each phosphor and the second using the best linear fit following the first calibration (see Ref. 8). The fully calibrated contrast of each phosphor was correct to within 0.017 log unit.

B. Stimuli

All stimuli were two-dimensional, circular blobs that were Gaussian enveloped in both dimensions of space ($\sigma = 0.35$ deg) and in time ($\sigma = 88$ ms). The small size and brief presentation ensured that the overall state of adaptation of the observer was not affected by the presentation of the stimulus. The spatial envelope was generated by frame-by-frame, pixilated dithering, which was visible at high luminance contrasts but which was easily ignored by the observer. The stimuli were presented in the center of the screen display (26×30 cm, 11×11 deg, 672×750 pixels), which was otherwise filled by a fixed white background illumination [CIE (0.33, 0.31), 55 cd m^{-2}]. A small, dark fixation spot was placed in the location of the stimulus display.

C. Color Space

We used a color space defined by the three cardinal axes.[9] Each axis lies in the unique direction that stimulates one of the detection mechanisms (red–green, blue–yellow, luminance) in isolation. We defined these axes as a linear transformation of long, medium, and short (L, M, and S)-wavelength-sensitive cone-contrast space. For all three subjects tested, the blue–yellow and luminance axes were fixed in the S-cone and L + M + S directions of cone-contrast space, respectively. To obtain a red–green cardinal axis that was truly isoluminant, a minimum-motion adjustment was performed by each subject within the plane defined by the L–M and L + M + S directions.[2] The stimulus was a 1-c/deg grating drifted at 1 Hz, comparable to our 1.4-deg, 350-ms spots (measured between ± 2 standard deviations). For each subject, the cardinal axes were scaled in units of detection threshold. For this purpose, repeated (4–8) measurements of contrast threshold were performed for stimuli in each of the three cardinal directions for each subject.

Within the (rg, by, lum) space defined by the cardinal axes, a stimulus vector was denoted by using a spherical coordinate system.[10] The vector magnitude defined the stimulus contrast (at zero contrast, the stimulus was identical to the background white). The angle between the stimulus vector and the isoluminant (rg–by) plane was called the stimulus elevation. The angle to the red–green axis of the vector projection on the isoluminant plane was termed the stimulus azimuth. The axis directions were denoted separately as the red (r) and green (g) cardinal directions (red–green axis), the blue (b) and yellow (y) cardinal directions (blue–yellow axis), and the light (l) and dark (d) cardinal directions (luminance axis).

D. Procedure

The detection thresholds of various test components T were measured using a two-alternative forced-choice procedure. Each presentation consisted of three stimuli displayed one after the other. Two stimuli were the fixed pedestal alone (P); the other stimulus (presented either first or third in the three-stimulus sequence) was the pedestal-plus-test combination ($P + T$). The color direction of P and T was fixed in each staircase and the contrast of T was adjusted between trials. The observer's task was to detect which presentation (the first or third) contained the test. The fixed reference stimulus (presented second) was used to ensure that the observer not only saw a difference between P and $P + T$ at threshold but was also able to determine which stimulus actually contained the test. All three stimuli were of 500-ms duration, with 125-ms inter-stimulus intervals. Audio feedback was provided. A staircase procedure was used: Threshold was determined by the average of the last six of eight staircase reversals. This measured threshold converged at the 81.6% correct level. An average of between three and six staircase measurements was used to obtain each threshold value.

E. Paradigms

Two paradigms were used. In both paradigms, the pedestal was fixed in one of several (ten to twelve) directions in both the rg–lum and the by–lum planes of cardinal space. In the first paradigm (Fixed Test Direction—Experiment 1), the test direction was fixed in a direction perpendicular to that of the pedestal in cardinal space [Fig. 1(a)]. For each fixed pedestal direction, test thresh-

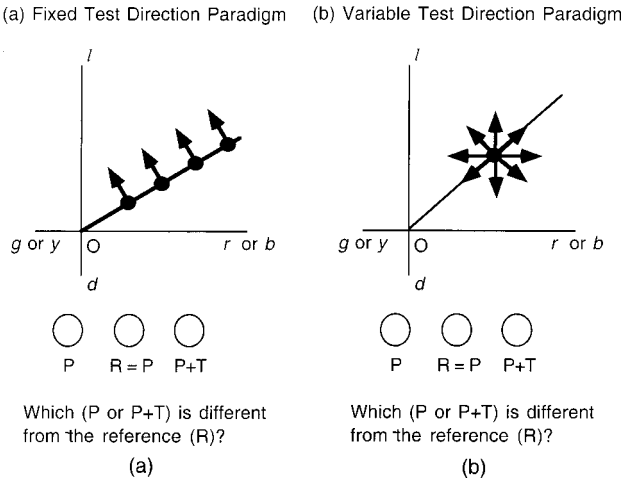

Fig. 1. Experimental paradigms. (a) In the Fixed-Test-Direction Paradigm, the direction of the pedestal (solid line) is fixed in a given plane (rg–lum or by–lum), while that of the test is fixed in a direction orthogonal to the pedestal (arrow). The test threshold is measured as a function of pedestal contrast. (b) In the Variable-Test-Direction Paradigm, the direction and magnitude of the pedestal are fixed (spot on solid line). The test threshold is measured as a function of test direction.

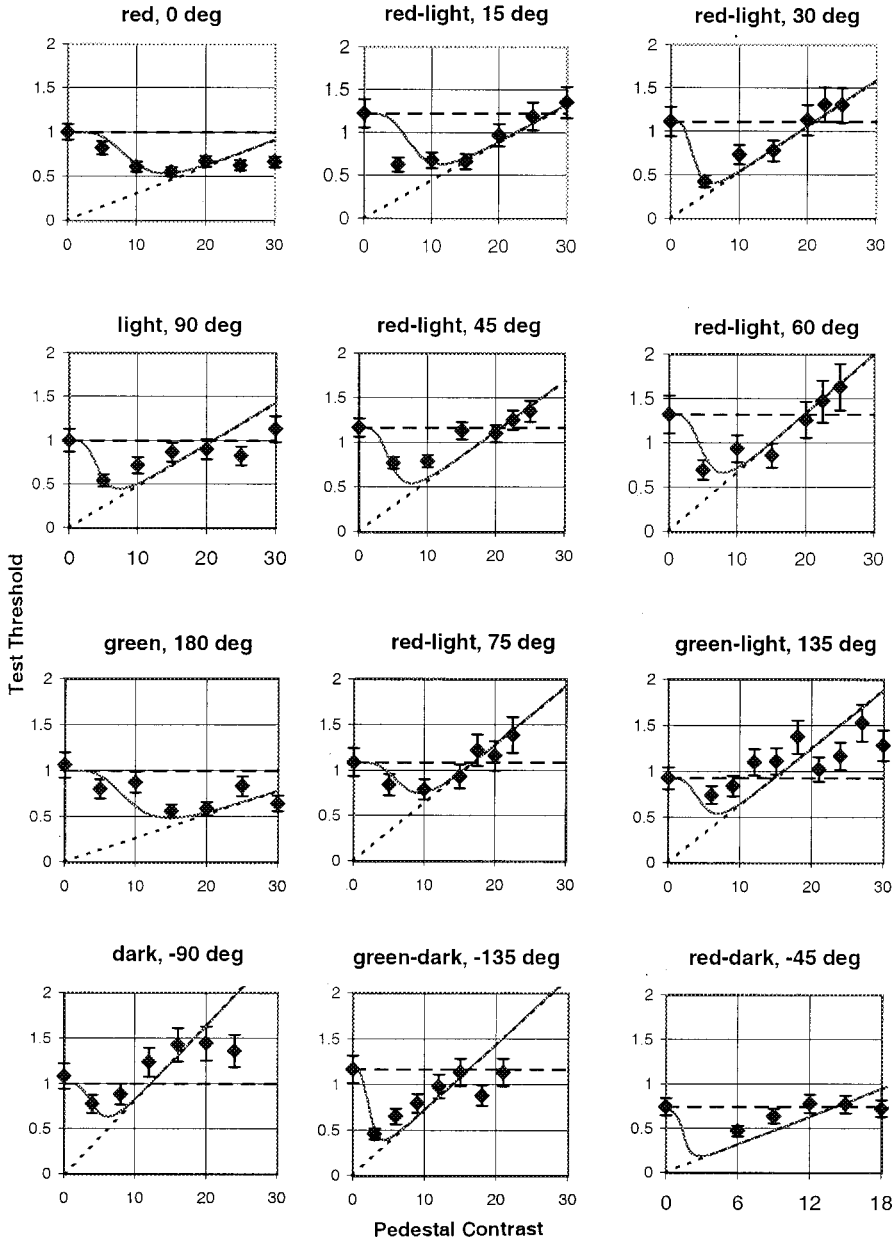

Fig. 2. Hue-increment detection thresholds in the rg–lum plane for subject MJS. Each panel represents one pedestal direction (shown at the top of the panel). The pedestal angle (deg) is relative to the red axis. The diamonds (with standard error bars) represent measures of test threshold with pedestal contrast. The solid curves represent the ratio model fit. The two asymptotes of the fit are the line $T = T_0$ (horizontal dashed lines), where T_0 is the measured value of test threshold at $P = 0$, and the line $T = P/\Delta$ (sloping dashed lines), where Δ is a fitted parameter. Note that the sloping asymptote is confined to pass through the origin.

old was measured as a function of pedestal contrast. In the second paradigm (Variable Test Direction—Experiment 2), the pedestal remained fixed in both contrast and direction, and the test threshold was measured as a function of test direction [Fig. 1(b)].

F. Observers

The three authors participated as observers in these tests. All had normal color vision (Farnsworth–Munsell 100 test), and all wore their normal refractive corrections. The observers were tested monocularly with free viewing at 150 cm.

3. RESULTS

A. Experiment 1: Fixed Test Direction

The results for the first paradigm are shown in Figs. 2–5. Each figure shows the results for one cardinal plane (rg–lum or by–lum) for one subject. These are, in order, the rg–lum plane for subjects MJS (Fig. 2) and KTM (Fig. 3) and the by–lum plane for subjects MJS (Fig. 4) and TJH (Fig. 5). Each panel contains the data for one pedestal direction, indicated in bold type at the top of each panel. Thus the top-left panel of Fig. 2 shows the result for the pedestal along the red cardinal axis, whereas the top-middle panel shows the result for the pedestal in the red-

light quadrant at an angle of 15 deg to the red axis. The four panels in the left-hand column of each figure contain the results for the four cardinal directions in each plane. In each panel, the horizontal axis represents the pedestal contrast, while the vertical axis shows the test threshold. These are scaled in the cardinal units described in Subsection 2.C and therefore represent multiples of thresholds along the cardinal axes. The diamonds represent the measured test thresholds with standard errors (averaged in log units within each panel). In each panel, the leftmost point (on the vertical axis) represents the test threshold in the absence of a pedestal. Ideally, from the definition of the cardinal axes, these zero-pedestal thresholds were equal to one for pedestals fixed in one of the cardinal directions. In practice, these thresholds were remeasured as part of the test data set.

We test the application of a ratio model using a fit that embodies this model at high pedestal contrasts (solid curves), described in Appendix A. This fit consists of three parts: (1) a short, low-pedestal-contrast segment that passes through the zero-pedestal threshold and remains constant with pedestal contrast; (2) a long, high-pedestal-contrast segment constrained as a line passing through the origin; and (3) an ogive-shaped transition between the previous two segments. This fit was chosen for its parsimony, since only two fitted parameters are required: the slope ν of high-pedestal-contrast segment, and the pedestal contrast π representing the midpoint of the transitory segment. The values of these fitted parameters are shown in Table 1. This table contains the results within each plane (rg–lum, by–lum) along with the previously obtained results in the isoluminant (rg–by) plane.[8] The values of π average 4.9 ± 2.0 (rg–lum) and 6.2 ± 2.0 (by–lum), consistent with the value of 5.1 ± 1.5 previously obtained for the (rg–by) plane.[8] In this table we represent the slope ν by its reciprocal $\Delta = 1/\nu$, termed the discriminability index. The value of this index increases with discrimination sensitivity. Also tabulated is the goodness-of-fit parameter Q (see note below Table 1), which varies from zero (no fit) to one (perfect fit). The table and figures show that the ratio model is a good fit ($Q > 0.1$; see Ref. 11) for most of the pedestal directions used. The exceptions to this (shown by boldface type in the table) typically arise for pedestal, and there-

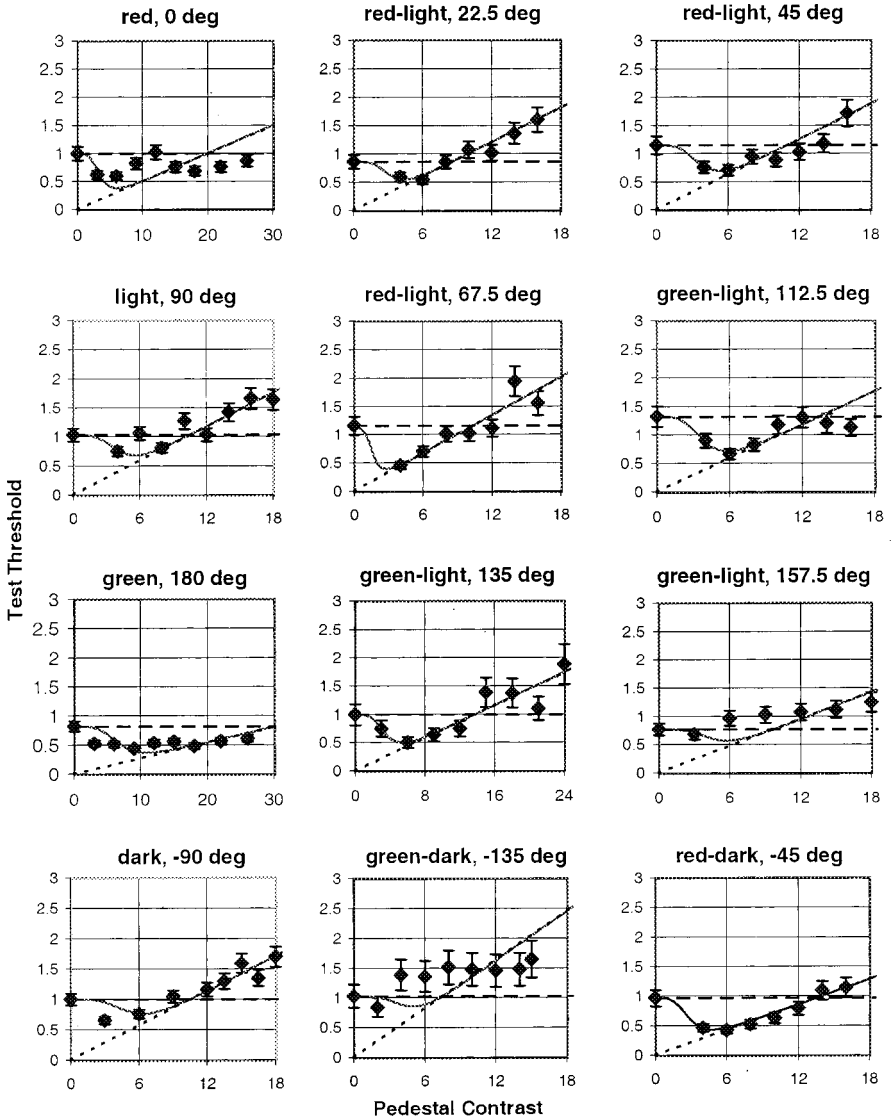

Fig. 3. Hue-increment detection thresholds in the rg–lum plane for subject KTM. See caption for Fig. 2.

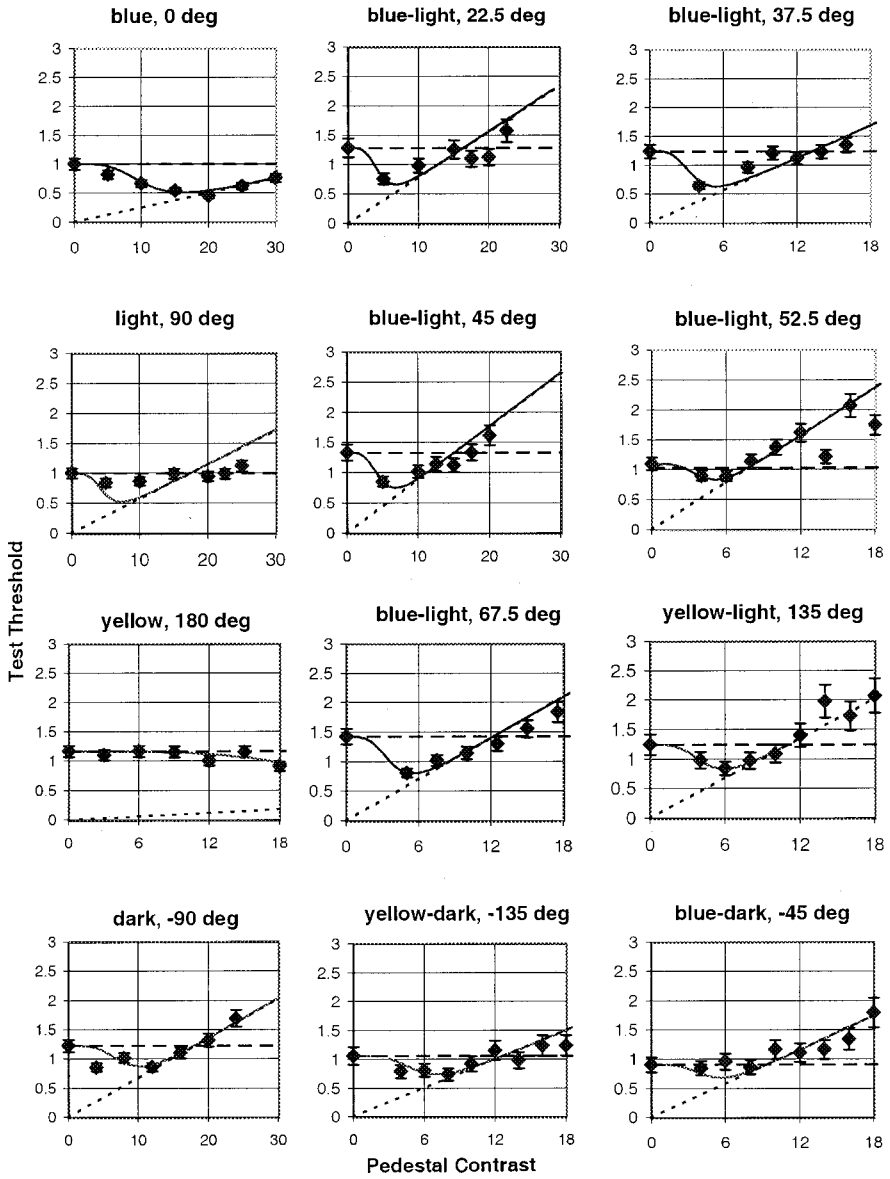

Fig. 4. Hue-increment detection thresholds in the by–lum plane for subject MJS. The pedestal angle (deg) is relative to the blue axis. See caption for Fig. 2.

fore test, directions lying parallel to the cardinal axes. This result may point to the presence of additional processes mediating discrimination of differences uniquely discernible by a single cardinal mechanism.

B. Experiment 2: Variable Test Direction

The results for the second paradigm are shown in Fig. 6. Each panel shows the result for one plane for one subject; for instance, in the top-left panel, the data for the rg–lum plane for subject MJS is shown. The axes represent the cardinal axes defining the plane. The four x symbols (one in each quadrant) represent the four fixed pedestals in this plane (see figure caption). These were fixed at oblique (45 deg) directions in each quadrant at the maximum allowable pedestal contrast for each subject (10 for MJS and TJH; 8 for KTM). The triangles encircling the origin represent the test thresholds in the absence of any pedestal, and those encircling each x symbol represent a translation of these data by the vector representing the fixed pedestal in each condition.

The circles represent the measured test thresholds as a function of test direction for each fixed pedestal. In accordance with a simple model of suprathreshold discrimination, each test-threshold contour was fitted by an ellipse.[12] From these fits, we observed that the aspect ratio of these ellipses averaged 2.5 (range 1.2–2.8). The orientations of the ellipses are shown graphically in Fig. 7. Two features are observed from this figure. First, the orientations are less than 45 deg, indicating that the chromatic component of the pedestal has a greater masking effect than the luminance component. Second, the orientations are generally lower for pedestals in the dark hemiplane ("darkish": elevations between 180 and 360 deg) than for pedestals in the light hemiplane ("lightish": elevations between 0 and 180 deg). Both observations are confirmed by statistical analysis. The two-standard-

deviation limit (95% CI) of the orientation for each of the two planes lies completely below 45 deg (28.1–44.6 deg, rg–lum; 19.7–42.0 deg, by–lum), and a two-treatment analysis-of-variance test (t test) shows that the orientations for darkish pedestals are significantly less ($p = 0.02$) than those for the lightish pedestals.[13] Both results suggest that suprathreshold discrimination of the luminance component may be more sensitive than that of each chromatic component.

4. DISCUSSION

We observed that a ratio model provides a good description of increment thresholds as a function of pedestal contrast for a wide range of pedestal contrasts. An attractive feature of this model is that it requires only one free parameter (the constant of proportionality), given our finding that the transition pedestal contrast is consistently near five times pedestal-contrast threshold. A second property of the model is that it can account partially for facilitation (see below) and masking. The model is consistent with a recently proposed five-stage process of discrimination of chromoluminant discrimination.[5] The first two processes are cone transduction and three-mechanism postreceptoral detection, which are the same as those assumed to exist in the present study. The third stage, similar to the ratio model proposed here, is a postulated divisive inhibition, in which each output of the three detection mechanisms are normalized by a summed response from all three mechanisms. We note that in the case where stimuli affect only two detection mechanisms at a time, as in our experiments, this normalization reduces approximately to a ratio model (Appendix B).

We suggested in our previous study that discrimination might be the direct result of the extraction of a ratio of postreceptoral-mechanism responses. This aspect of our hypothesis contradicted the multistage model, which argued for divisive inhibition from a powered sum of all three postreceptoral responses. Our hypothesis of a direct ratio extraction was founded on two observations: (1) that the discriminability parameter Δ was constant over each plane of color space and (2) that the introduction of a pedestal-contrast increment did not affect the de-

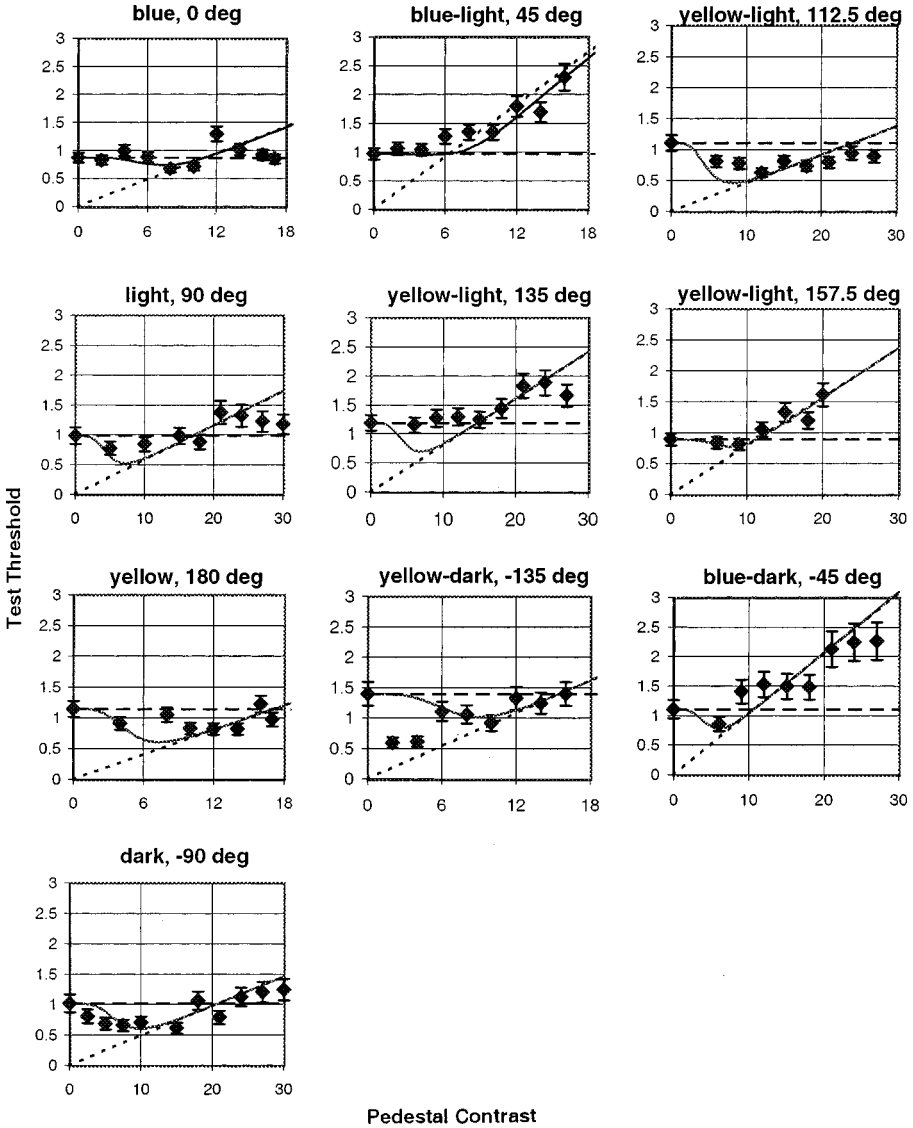

Fig. 5. Hue-increment detection thresholds in the by–lum plane for subject TJH. The pedestal angle (deg) is relative to the blue axis. See caption for Fig. 2.

Table 1. Fitted Parameters for the Ratio Model in the Three Cardinal Planes[a]

	(rg–by)						(rg–lum)						(by–lum)				
	θ	N	π	Δ	Q		θ	N	π	Δ	Q		θ	N	π	Δ	Q
MJS	0	7	4.6	15.0	0.38	MJS	0	7	9.8	33.0	0.62	MJS	**0**	**7**	**5***	**34.1**	**0.01**
	10	7	5*	19.7	0.10		15	7	7.7	22.6	0.84		23	7	4.7	12.8	0.84
	23	7	4.3	9.4	0.78		30	7	3.6	18.9	0.92		30	9	9.7	13.6	0.95
	35	7	4.4	8.9	0.79		45	7	5.0	17.8	0.30		38	7	3.6	10.7	0.77
	45	7	4.4	8.6	0.28		60	7	5.3	15.0	0.65		45	7	4.8	11.3	0.95
	68	7	4.0	10.8	1.00		75	7	7.7	15.6	0.96		53	9	4.5	7.6	0.96
	80	7	5.4	20.8	0.46		**90**	**7**	**4.7**	**21.0**	**0.09**		60	9	6.1	8.2	0.96
	90	7	6.8	21.4	0.93		135	10	6.8	15.9	0.70		68	7	3.9	8.6	0.93
	135	7	3.9	9.5	0.11		**180**	**8**	**5***	**29.9**	**0.03**		**90**	**7**	**5***	**17.4**	**0.08**
	180	8	5*	23.8	0.47		−135	8	2.5	13.9	0.74		135	9	4.7	8.9	1.00
	−135	7	3.9	11.0	0.37		−90	7	4.8	12.2	0.17		180	8	5*	12.0	0.41
	−90	8	5*	13.2	0.24		−45	10	4.4	19.1	0.93		−135	9	5.9	12.0	0.99
	−45	7	5.7	18.0	0.84								−90	8	8.7	14.7	0.89
						KTM	**0**	**9**	**3.6**	**13.6**	**0.00**		−45	9	5*	10.3	1.00
KTM	**0**	**7**	**5***	**21.7**	**0.00**		23	8	3.4	9.9	0.94						
	23	7	5.9	6.9	0.92		45	8	3.9	9.6	0.96	TJH	0	10	7.5	12.6	0.61
	45	6	5.2	4.5	0.86		68	8	1.6	8.9	0.28		23	8	3.6	9.0	0.73
	68	7	5.9	6.8	0.98		90	9	4.4	10.2	0.94		45	9	9.2	6.6	0.96
	90	7	5.9	8.8	0.23		113	8	4.0	10.2	0.98		68	8	6.0	10.0	0.98
	113	7	7.5	8.4	0.89		135	9	3.6	13.8	0.99		90	9	5*	17.3	0.72
	135	7	4.8	11.6	1.00		158	8	5*	12.6	0.41		113	9	5*	21.8	0.76
	168	7	4.7	14.1	0.87		180	9	7.0	37.1	0.34		135	9	5*	12.4	0.43
	180	**7**	**5***	**23.8**	**0.05**		−135	9	5*	7.3	0.21		158	7	8.4	12.6	0.48
	−168	7	4.3	13.9	0.84		−90	9	5.7	10.5	0.96		180	8	5*	15.0	0.90
	−135	7	1.9	7.3	0.98		−45	8	3.1	14.5	1.00		−135	9	7.7	11.1	0.70
	−113	6	4.1	8.3	0.55								−90	11	7.3	20.5	0.99
	−90	6	9.4	5.2	0.79								−45	9	5*	9.7	0.92
	−68	6	5.4	16.6	0.97												
	−45	7	6.6	15.0	0.83												
	−23	7	5*	19.2	0.93												

[a] The parameters in the (rg–by) plane were obtained from our previous study.[8] θ, pedestal direction in degrees within the plane (rg–by: $r = 0$, $b = 90$; rg–lum: $r = 0$, $l = 90$; by–lum: $b = 0$, $l = 90$); N, number of threshold measurements; π and Δ, fitted parameters (see Appendix A). The asterisks (*) in the π column indicate values of π that in the best fit were suspected outliers resulting from fit degeneration (a criterion value of $\pi > 10.0$ was used). These values were excluded from the averages quoted in the text and, for the sake of plotting and determining the quoted value of Δ, were artificially set to five. Q is the goodness of the fit, calculated as the likelihood of obtaining the measured χ^2 value of each fit of the ratio model. $Q = 1$ implies a perfect fit ($\chi^2 = 0$), and $Q = 0$ implies that the measurements do not obey the model. The acceptability criterion was chosen to be $Q > 0.1$ (Press *et al.*[11]). The table shows that the ratio model is a good fit to the measured test-threshold data except in seven cases (bold type), for all of which the pedestal and test lie along the cardinal axes ($\theta = 0$, 90, 180, or −90 deg).

tection of the test. If a more complex divisive inhibition were involved, we would expect that, in the first place, there would be a systematic shift in Δ as one of the cardinal axes was approached and, in the second instance, that the introduction of a pedestal contrast increment would affect the detection of the test. We now test the first condition, namely, the uniformity of discriminability within the rg–lum and by–lum planes (Fig. 8). In this figure, the data points (*) for each measurement in the fixed-test-direction paradigm are shown in their correct positions in each color plane. The proportionality relationship given by the application of the ratio model in each case is represented by a discrimination zone (shaded). Hence the width of each shaded zone is proportional to the limit of discrimination predicted by the ratio model. We perform a statistical test[14] to determine whether these zones are uniformly wide within each plane for each subject. The results of this test show that the model stating that these widths are uniform is supported by high-likelihood values in the rg–lum plane for both subjects ($Q = 0.97$, MJS; 0.96, KTM) and in the by–lum plane for one subject (0.86, MJS). The uniformity model was not supported for one subject in the by–lum plane ($Q < 0.1$, TJH), due largely to one aberrant result[15] in the light-yellow quadrant (pedestal angle = 112.5 deg). Any observed uniformity suggests that a direct ratio extraction is to be favored over a divisive process involving inhibition of each mechanism by its own response. A more important ramification of zone uniformity, however, is the use of cardinal coordinates itself. This is because uniformity is sensitive to the choice of these axes, in both magnitude and direction (see Ref. 16). Thus the presence of uniformity suggests that a space defined by threshold-scaled cardinal axes is appropriate for modeling suprathreshold interactions. This finding suggests, in turn, that the mechanism of suprathreshold discrimination depends

primarily on the responses of the three postreceptoral mechanisms normalized relative to their individual detection thresholds.

With one notable exception (KTM, rg–lum plane for light and dark pedestals), we observed a failure of the ratio model when the pedestal and test directions lie along the cardinal axes. This extends our previous finding in the isoluminant plane.[8] We postulate that this characteristic can be accounted for by an ability of the postreceptoral mechanisms to detect cardinal test increments directly. This functional independence among the postreceptoral mechanisms for spot stimuli has been observed in previous cross-luminance/red–green pedestal experiments.[17]

Our results suggest, at least for noncardinal tests, that there are two processes involved: (1) detection of the test alone at low pedestal contrasts, (2) discrimination based on an inhibitory process at high pedestal contrasts. The inhibitory process is confined to relatively high pedestal contrasts, and this is consistent with the perceptual phenomenon that close hues are difficult to distinguish near detection threshold. At high pedestal values, the inhibitory process determines discrimination, and thresholds based on the test alone appear suppressed. In perceptual terms, this finding implies that hue-based discrimination is used even when detection of the test alone may be available.

The inhibitory process can account for both test thresh-

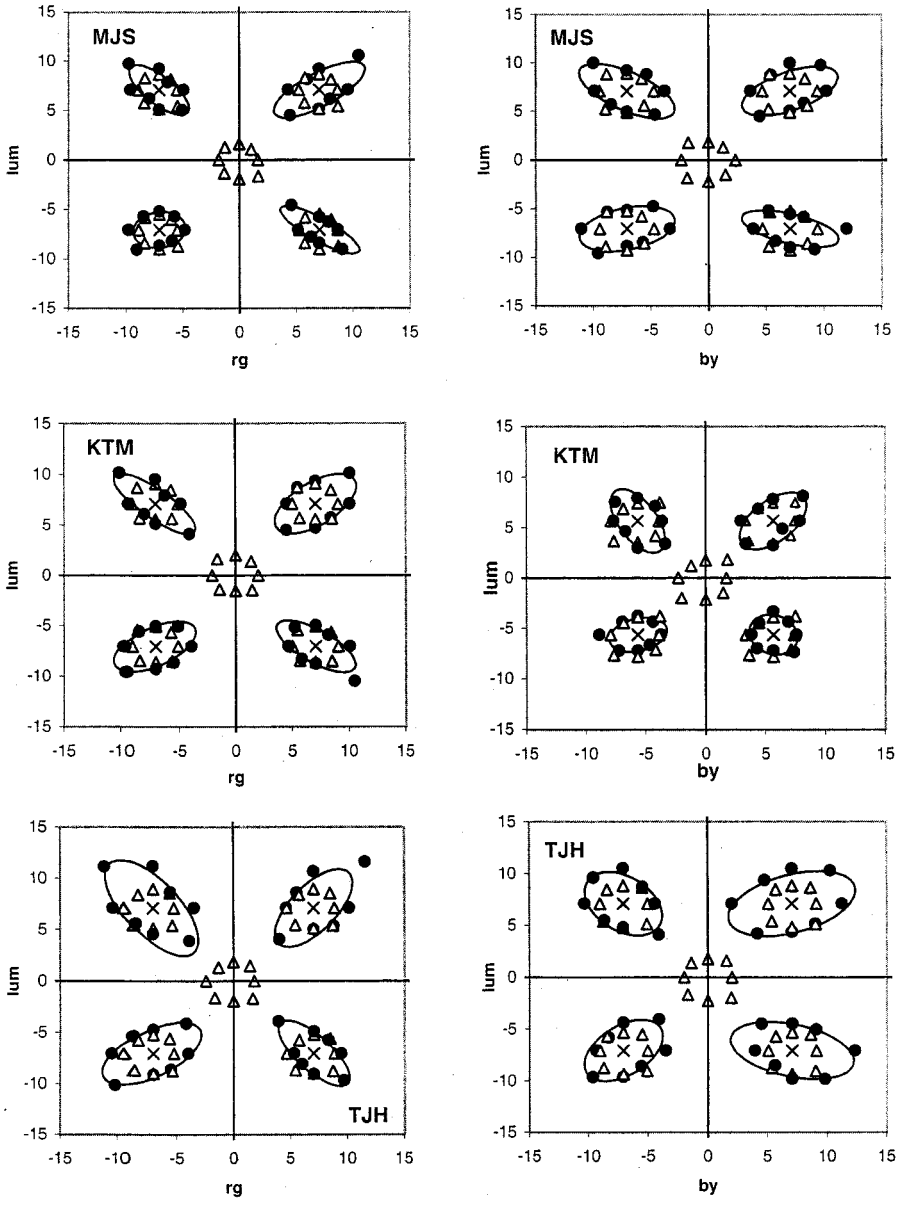

Fig. 6. Results of variable-test-direction paradigm. Each panel represents one plane for one subject. The pedestal was fixed in one of four positions (X) in the plane (the coordinates of the pedestal have been scaled by 0.5 for the purposes of the graph). Circles represent the test threshold as a function of test direction for each of the four pedestal values in each plane. Triangles encircling the origin represent the test thresholds in the absence of a pedestal. Triangles encircling each of the four pedestal values are a translation of these test thresholds. Comparison of the circles and the triangles around each pedestal value yields an elongation of the test-threshold contour in the presence of the pedestal. The elliptical fit to this contour (solid lines) shows that the maximum elongation occurs in a direction less than 45 deg from the horizontal (rg or by) axis. This may suggest that the elongation is a result of masking due to the pedestal and a small facilitation along the direction of the luminance axis.

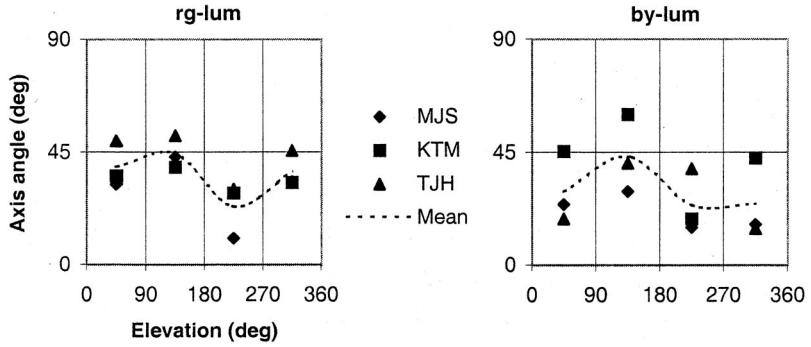

Fig. 7. Orientations of the major axes of the fitted ellipses. The two panels represent the two planes (rg–lum and by–lum). The horizontal axis represents the pedestal direction in each plane (a 0–360 deg representation has been used for convenience). 0 deg represents the red and blue axes in left and right figures, respectively. 90 deg represents the light axis. The vertical axis represents the absolute value of the angle between the major axis of the fitted test-threshold contour at each pedestal value and the chromatic (rg or by) cardinal axis. Symbols show the fitted orientations for each pedestal for each subject. Dashed curves represent the average orientation over the three subjects tested. The figure shows that the mean elongation is maximum at an angle less than 45 deg from the chromatic axis. This demonstrates that luminance discrimination is more sensitive than chromatic (isoluminant) discrimination with these pedestals and may indicate a direct contribution of the luminance mechanism in discrimination.

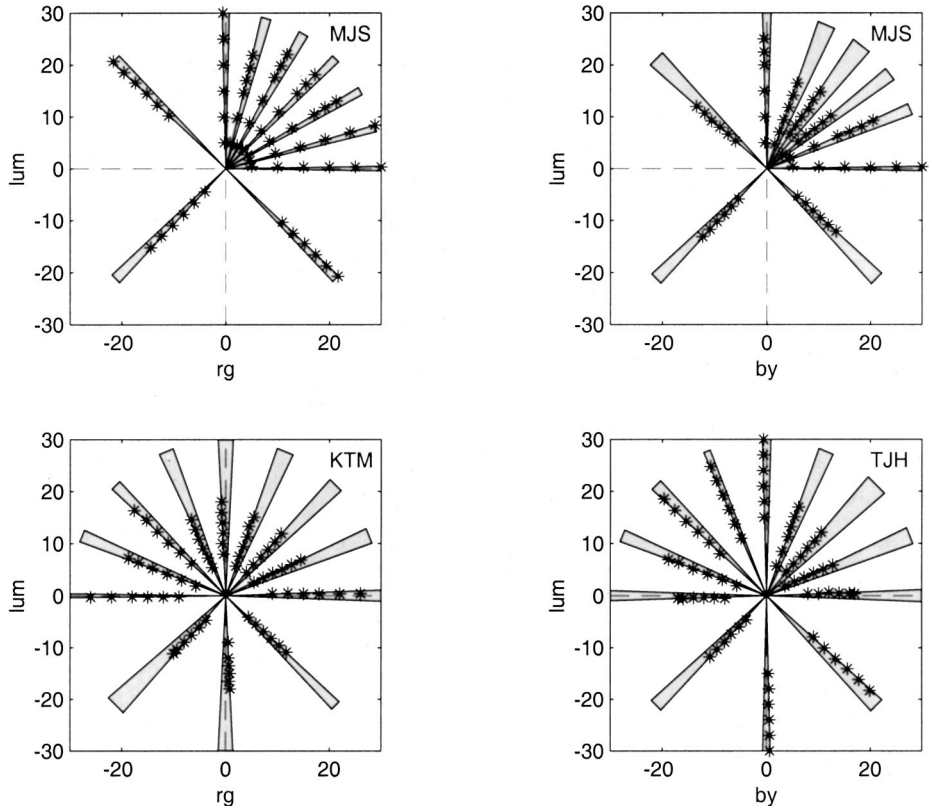

Fig. 8. Zone plots for discrimination (fixed-test-direction paradigm). Asterisks (*) represent the measurements of test threshold for each pedestal direction and contrast (obtained from Fig. 2–5). Shaded zones represent the region of discriminability for each pedestal direction (the bisector of the zone), as predicted by the ratio model (the width of the zones and the offset of the test threshold points from the pedestal axis have been halved for graphical clarity). The figure shows that, apart from along the cardinal axes and the 112-deg direction in the by–lum plane for subject TJH, the widths of the zones are uniform within each plane for each subject.

old facilitation at low pedestal contrasts and masking at high pedestal contrasts. Both features have been observed in numerous studies that used grating or spot pedestals or added noise.[3,4,18] Our results show that predominant activity of the inhibitory process is achieved at a critical suprathreshold pedestal contrast (approximately five times pedestal threshold). Thus, facilitation may arise when, for pedestals even lower than this critical value, detection by such mechanisms contributes to that of the test alone. The presence of masking, on the other hand, implies that detection of the test by the inhibitory process dominates that of the test component alone at high pedestal contrasts. These possibilities do not, of course, preclude the presence of other processes mediating facilitation, masking, or both. For example, the inhibitory process cannot account for facilitation and masking when the test and pedestal are fixed along the same axis. We also note that the processes underlying

noise masking may be different from those mediating increment detection for grating or spot pedestals: For instance, the degree of facilitation for tests and pedestals in cardinal directions is much lower in noise masking.[19] This reduced facilitation suggests that noise masks are less optimal for the inhibitory process and consequently that this process is primed when the spatial patterns of test and pedestal are similar. In addition, Chen *et al.*[6] observed a pattern of facilitation different from that obtained in the present study. They observed that facilitation did not occur for cardinal luminance tests or cardinal blue–yellow pedestals. They also discovered that masking (elevation above zero-pedestal threshold) occurred in all cases—even in the cases where the test was in one of the three cardinal directions. This was true despite the fact that their studies investigated a range of pedestal contrasts similar to those used in the present study. It is possible that the differing patterns of facilitation and masking result from the use of different spatiotemporal stimulus parameters between the two studies. Specifically, Chen *et al.*'s use of larger stimuli may favor the inhibitory process. In our results, the exceptional occurrence of masking for subject KTM for light and dark pedestals (rg–lum plane) may also suggest a subject dependence on this preferential tuning.

Our findings are consistent with our previous observations for stimuli constrained in the isoluminant plane.[8] Previous results using masking and detection differ on the question as to whether there exist significant differences between purely isoluminant processing and processing involving a luminance component. For instance, Wandell[7] showed that discrimination ellipses similar to those shown in Fig. 6 are different for the isoluminant and the nonisoluminant planes. Our results suggest that these differences do not appear in discrimination where the overall pedestal-plus-test contrast is kept approximately constant, as is the case in the Fixed-Test-Direction paradigm. However, when this overall contrast is altered, as in the Variable-Test-Direction paradigm, there may be significant differences between processing of the luminance and of the chromatic contrast components. From our observations, discrimination in these cases is better in the presence of luminance differences as opposed to changes in the purely chromatic component (axis angle less than 45 deg, Fig. 7). This may agree with Wandell's hypothesis that joint chromatic–achromatic discrimination in situations of variable overall contrast is performed by categorization within labeled regions of color space. Our observations may also reflect that achromatic changes (changes of shade) are more easily discriminated than isoluminant changes in normal vision for interpreting cast shadows, light reflections, and clear transparency. Indeed, the observed preferential discrimination for dark shades implies a role of such discrimination in, for example, shape from shading, where the shading (as the name implies) occurs as a luminance decrement with respect to the prevailing scene.

Our results as a whole provide a link between the red–green, blue–yellow, and luminance mechanisms that are responsible for detection and the multiple processes that mediate several aspects of color vision at suprathreshold level (e.g., hue discrimination, adaptation, color-guided search, motion coherence[20–22]). However, our model does not claim to explain precisely how these suprathreshold processes are formed, how they are organized within the visual system, or how they subserve more complicated color-based tasks. Within its current scope, our model is principally a descriptive tool that permits a systematic investigation of all these aspects of suprathreshold chromatic mechanisms.

APPENDIX A: THE RATIO MODEL

The model assumes that the test increment threshold T is proportional to the pedestal contrast P, for P greater than a certain switching value. There are two fitted parameters: the proportionality constant $\nu = 1/\Delta$ and the switching pedestal contrast π. The model takes the form

$$T = k_1 T_0 + k_2(P/\Delta), \tag{A1}$$

$$k_1 = \frac{\pi^4}{P_4 + \pi^4}; \qquad k_2 = 1 - k_1, \tag{A2}$$

where T_0 is the measured test threshold in the absence of a pedestal. By this definition, $T \cong T_0$ for $P \ll \pi$, and $T \cong P/\Delta$ for $P \gg \pi$; where $P = \pi$ is the value of P at which T lies vertically equidistant from the two asymptotes $T = T_0$ and $T = P/\Delta$.

APPENDIX B: THE RATIO MODEL AND DIVISIVE INHIBITION

The divisive inhibition of Chen *et al.*[6] takes the form

$$R_i = \frac{{m_i}^p}{\sum_{j=1}^{N} (a_{ij} {m_j}^q) + Z}, \tag{B1}$$

where R_i is the response of the ith mechanism following inhibition by all N postreceptoral mechanisms (including self-inhibition), m_i is the preinhibition postreceptoral mechanism response, a_{ij} is a fixed scaling factor, Z is a fixed inhibition component, and p and q are constant exponents. For two mechanisms, and for $p \cong q$, a criterion response C_R is achieved in each mechanism when

$$C_R = \frac{{m_1}^p}{a_{11}{m_1}^p + a_{12}{m_2}^p + Z}. \tag{B2}$$

If Z is sufficiently small, the above equation leads to

$$m_1/m_2 = C_R^{(1)}, \tag{B3}$$

which is the formulation of the ratio model.

ACKNOWLEDGMENT

This research was funded by Medical Research Council of Canada grant MT-10819 to K. T. Mullen.

Author contact information: Kathy Mullen, McGill Vision Research, 687 Pine Avenue West (H4-14), Montreal, Quebec H3A 1A1 Canada; e-mail, kathy.mullen@mcgill.ca (corresponding author). Marcel Sankeralli: e-mail, sankeram@magellan.umontreal.ca. Trevor Hine: e-mail, t.hine@mailbox.gu.edu.au.

REFERENCES

1. M. Gur and V. Akri, "Isoluminant stimuli may not expose the full contribution of color to visual functioning: spatial contrast sensitivity measurements indicate interaction between color and luminance processing," Vision Res. **32**, 1253–1262 (1993).
2. K. T. Mullen and M. J. Sankeralli, "Evidence for the stochastic independence of the blue–yellow, red–green and luminance detection mechanisms revealed by subthreshold summation," Vision Res. **39**, 733–743 (1999).
3. E. Switkes, A. Bradley, and K. K. Devalois, "Contrast dependence and mechanisms of masking interactions among chromatic and luminance gratings," J. Opt. Soc. Am. A **5**, 1149–1162 (1988).
4. G. R. Cole, T. J. Hine, and W. H. MacIlhagga, "Estimation of linear detection mechanisms for stimuli of medium spatial frequency," Vision Res. **34**, 1267–1278 (1994).
5. C.-C. Chen, J. M. Foley, and D. H. Brainard, "Detection of chromoluminance patterns on chromoluminance pedestals I: threshold measurements," Vision Res. **40**, 773–788 (2000).
6. C.-C. Chen, J. M. Foley, and D. H. Brainard, "Detection of chromoluminance patterns on chromoluminance pedestals I: model," Vision Res. **40**, 789–803 (2000).
7. B. A. Wandell, "Colour measurement and discrimination," J. Opt. Soc. Am. A **2**, 62–71 (1989).
8. M. J. Sankeralli and K. T. Mullen, "Ratio model for suprathreshold hue-increment detection," J. Opt. Soc. Am. A **16**, 2625–2637 (1999).
9. J. Krauskopf, D. R. Williams, and D. W. Heeley, "Cardinal directions of colour space," Vision Res. **22**, 1123–1131 (1982).
10. A. M. Derrington, J. Krauskopf, and P. Lennie, "Chromatic mechanisms in lateral geniculate nucleus of macaque," J. Physiol. (London) **357**, 241–265 (1984).
11. W. H. Press, S. A. Teukolsky, W. T. Vetterling, and B. P. Flannery, *Numerical Recipes in C: The Art of Scientific Computing*, 2nd ed. (Cambridge U. Press, Cambridge, UK, 1992).
12. The elliptical model presupposes that in the presence of a suprathreshold noncardinal pedestal, test threshold is determined by two distinct mechanisms: one detecting the test component parallel to the pedestal color direction (a contrast increment), the other detecting the component perpendicular to this direction (a hue increment). Our previous results supported this separation, at least for the isoluminant plane.[8]
13. In the single-variable, two-treatment analysis of variance (*t* test), the difference of the means of the two treatments was compared with the 95% acceptability level of the *t* parameter given the number of trials involved per treatment.
14. To determine whether the parameter Δ is constant within each plane, we performed a chi-squared test of the error across treatments (MST) compared with the error within each measurement (MSE). This analysis did not include data from the cardinal pedestal directions. MST is given by the standard error of the fitted mean Δ's; MSE is calculated from the width W of the 95% confidence interval for each fitted Δ: $\mathrm{MSE} = \mathrm{mean}\{(W/2)/t_{\alpha/2}\}$, where $t_{\alpha/2}$ is the t statistic at $\alpha/2 = 0.025$. The quantity $\chi^2 = \mathrm{MST/MSE}$ was used to compute a Q value—the probability that the variability in Δ could be accounted for by a random measurement variability. As in the main test, the variation in Δ was accepted as random (as opposed to a systematic departure from uniformity) if $Q > 0.1$.
15. It is possible that this pedestal direction lies near the actual "blue" cardinal pole for this subject.
16. M. J. Sankeralli and K. T. Mullen, "Assumptions concerning orthogonality in threshold-scaled versus cone-contrast colour spaces," Vision Res. **41**, 53–55 (2001).
17. G. R. Cole, C. F. Stromeyer III, and R. E. Kronauer, "Visual interactions with luminance and chromatic stimuli," J. Opt. Soc. Am. A **7**, 128–140 (1990).
18. K. T. Mullen and M. A. Losada, "Evidence for separate pathways for color and luminance detection mechanisms," J. Opt. Soc. Am. A **11**, 3136–3151 (1994).
19. M. J. Sankeralli and K. T. Mullen, "Postreceptoral chromatic detection mechanisms revealed by noise masking in three-dimensional cone contrast space," J. Opt. Soc. Am. A **14**, 2633–2646 (1997).
20. J. Krauskopf, D. R. Williams, M. B. Mandler, and A. M. Brown, "Higher order colour mechanisms," Vision Res. **26**, 23–32 (1986).
21. M. D. Zmura, "Color in visual search," Vision Res. **31**, 951–966 (1991).
22. J. Krauskopf, H.-J. Wu, and B. Farrell, "Coherence, cardinal directions and higher-order mechanisms," Vision Res. **36**, 1235–1245 (1996).